THE TOROIDAL LARGE-SCALE MAGNETIC FIELD OF THE SUN

V.M. Grigoryev, S.M. Latushko, V.S. Peshcherov
SibIZMIR, Irkutsk 33, P.O.Box 4, 664033 USSR

ABSTRACT. This work has utilized daily Stanford magnetograms for construc-
ting synoptic charts of distributions of the magnetic field toroidal and ra-
dial components. Also, charts were constructed of the distributions of field
line slopes in the E-W direction. We obtained new insights into the structure,
dynamics and interrelation of the toroidal and poloidal field components. The
distributions of (average in latitude over the period under study) toroidal
and radial fields are compared with values obtained in previous studies.

ТОРОИДАЛЬНОЕ КРУПНОМАСШТАБНОЕ МАГНИТНОЕ ПОЛЕ СОЛНЦА: В работе использова-
лись ежедневные магнитограммы Стенфордской обсерватории за период январь 1979 -
май 1981 для построения синоптических карт распределения тороидального и ра-
диального компонентов магнитного поля. Построены также карты распределения на-
клона силовых линий в E-W направлении. Получены сведения о структуре, динамике
и взаимосвязи тороидального и полоидального компонентов поля. Распределения
средних по широте за исследуемый период тороидального и радиального полей сра-
вниваются со значениями, полученными в предшествующих работах.

VEĽKOROZMERNÉ TOROIDÁLNE MAGNETICKÉ POLE NA SLNKU: Pre obdobie január
1979 až máj 1981, z denných magnetických máp Stanfordského observatória boli
vypočítané hodnoty toroidálnej a radiálnej zložky magnetického poľa Slnka.
Okrem toho bol určený sklon magnetických siločiar v smere E-W. Boli získané
nové údaje o štruktúre, dynamike a vzájomnom vzťahu toroidálnej a poloidálnej
zložky magnetického poľa. Stredné hodnoty toroidálnych a radiálnych zložiek,
vypočítané pre celé uvedené obdobie, sú porovnané s hodnotami obdržanými v
prácach iných autorov.

1. INTRODUCTION

The study of the large-scale magnetic field of the Sun is confined mainly

481

to the assumption about its radiality as well as to observations of the longi-
tudinal component of the full vector alone. In order to refine the extant mo-
dels of solar dynamo, and also those of the global field of the Sun, however,
requires information on the magnitude, structure and dynamics of the magnetic
field full vector. In this connection, a method has proved useful which is di-
rected at obtaining the toroidal and radial components from observations of
the longitudinal component of the full vector of magnetic field elements du-
ring their disk passage. Yet the method introduces a certain ambiguity in the
values of components obtained due to magnetic field evolution. Reliable re-
sults are obtainable only for large spatial and temporal averages (several so-
lar rotations). Thus, based on daily Mt.Wilson magnetograms for 1967-1973 Ho-
ward (1974) found that photospheric magnetic field lines during that period
were tilted (by about 0.8°) eastward in both hemispheres. Using an improved
technique for singling out the magnetic field toroidal component from longi-
tudinal component observations with low spatial resolution but very high sen-
sitivity (of about 0.05 Gs) the Stanford group (Duvall et al., 1979) obtained
a number of useful, reliable results on the latitude-time distribution of the
value of the magnetic field toroidal and radial components. Svalgaard et al.
(1978) obtained a picture of magnetic field line distribution in the polar
zones.

In addition to average (for long time intervals) characteristics of the
toroidal and radial magnetic fields, it is also of interest to study their la-
titude-longitude distribution and dynamics on shorter time scales. In this pa-
per, daily three-minute Stanford magnetograms for the period January 1979 -
May 1981 will be employed for constructing synoptic maps of distribution of
magnetic field toroidal and radial components. Also, maps of distribution of
field line inclination in E-W direction are constructed, and mean values of
the two components of the magnetic field found for the period under study.

2. DATA TREATMENT TECHNIQUE

The method we are using to single out the toroidal and radial components
of the magnetic field full vector from longitudinal component observations, is
basically the same as one suggested by Howard (1974) and Duvall et al. (1979).
The method relies on the quasi-constancy condition for the magnetic field full
vector, $\bar{H}$, for a selected point on the solar surface for the time it takes to
move from one disk edge to the other. This condition is satisfied reasonably
well for large-scale magnetic fields. Figure 1 illustrates how the method wor-
ks. Vector $\bar{H}$ is an arbitrary vector of magnetic field strength projected into
the equatorial plane. In cylindrical coordinates it decomposes into a radial
component H_r (the part symmetric about the central meridian) and into a toro-
idal component H_t (the antisymmetric part). The measured value of the longitu-
dinal field component H_1 is represented as

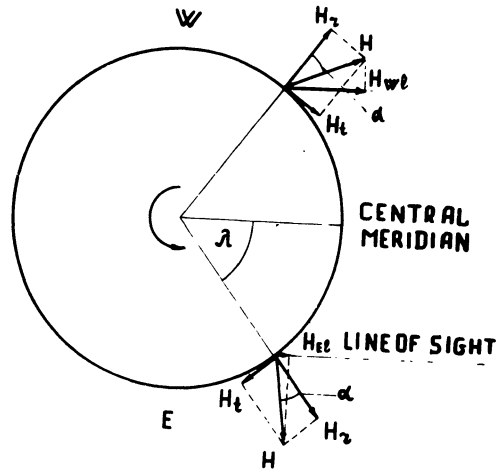$$H_{\ell} = H_{\lambda} \cos \lambda + H_t \sin \lambda \qquad (1)$$

Fig. 1: The various components of an arbitrary magnetic field vector on the
equatorial plane. The inclination of the solar rotation axis to the
ecliptic plane is neglected. λ is the solar longitude measured to the
east of the central meridian with the (-) sign. H_r is the radial
component of full vector $\bar{H}$ in cylindrical coordinates, with the axis
coinciding with that of solar rotation. H_t is the toroidal component
of the full vector. $H_{\ell E}$ and $H_{\ell W}$ is the full vector projected onto the
line of sight east- and westward of the central meridian, respecti-
vely.

where λ is the longitude which is considered positive westward of the central
meridian.

If one and the same element of the solar surface is observed at the same
longitude both east- and westward of the central meridian, then provided the
magnetic field is standard, the measured longitudinal component of field is
given by

$$H_{\ell E} = H_r \cos \lambda - H_t \sin \lambda \qquad (2)$$

$$H_{\ell W} = H_r \cos \lambda + H_t \sin \lambda \qquad (3)$$

where we may obtain

$$H_r = \frac{H_{\ell E} + H_{\ell W}}{2 \cos \lambda} \qquad (4)$$
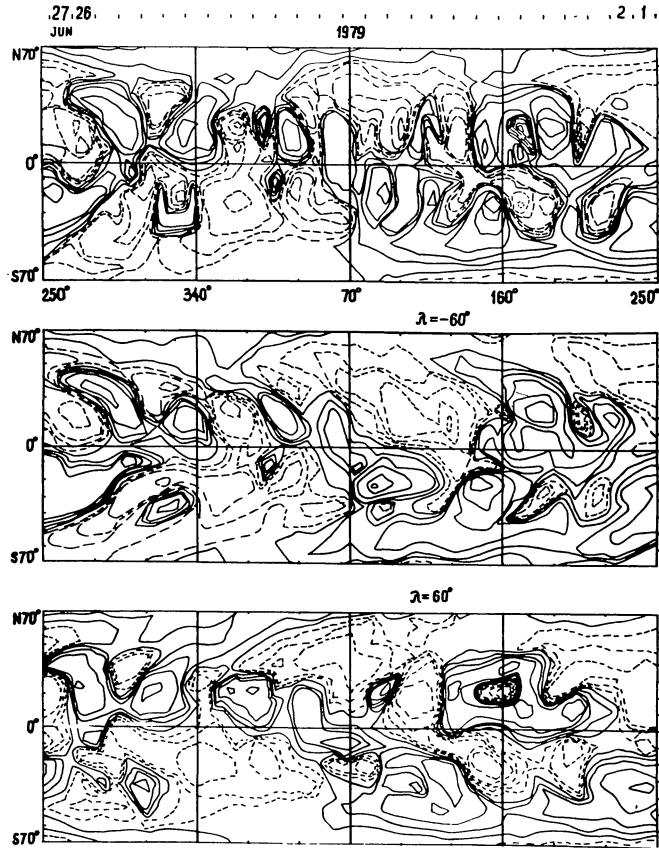
$$H_t = \frac{H_{\ell E} - H_{\ell W}}{2 \sin \lambda} \qquad (5)$$

483

Fig. 2: Synoptic maps of the magnetic field longitudinal component (Hℓ), constructed for heliographic longitudes L = 0°, L = -60° and L = 60°.

$$\tan \alpha = \frac{H_t}{H_r} = \frac{H_{\ell E} - H_{\ell W}}{H_{\ell E} + H_{\ell W}} \qquad (6)$$

where α is the angle between vector $\vec{H}$ and the solar radius. Daily magnetograms were used for constructing $H_{\ell W}$ and $H_{\ell E}$ synoptic maps for longitudes $\pm 60°$ from the central meridian, respectively (Fig. 2). The time delay for $H_{\ell W}$ is

$$\Delta t = T_{CR}/3$$

where T_{CR} is the Carrington period. Using, then, expressions (4) and (5) we constructed synoptic maps of the radial and toroidal components of the magnetic field for each solar rotation. That a toroidal component of the mean magnetic field does indeed exist is beyond doubt. Figure 3 presents the mean magnetic field measured as a function of longitude $H_\ell(\lambda)$ for the latitude zone
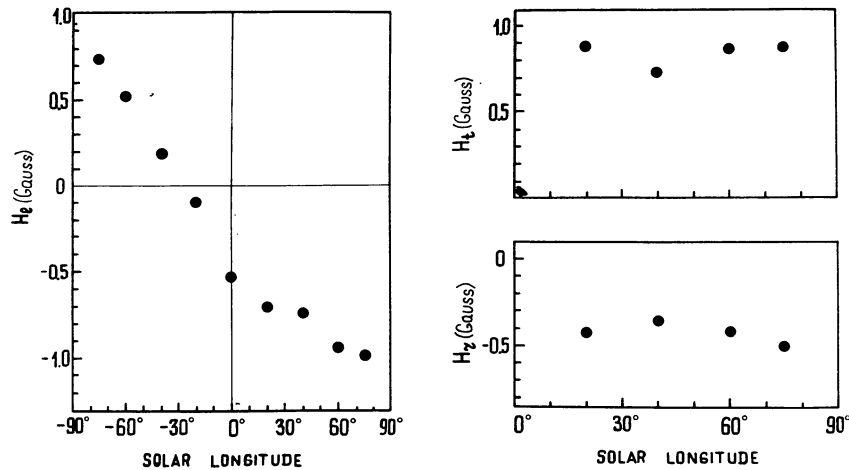
Fig. 3: The mean field, represented as a function of longitude for the lati-
tude zone $10°$ - $30°$S for 1-28 June 1979. The quantity H_{ℓ} is repre-
sented as $H_{\ell} = H_{r}\cos\lambda + H_{t}\sin\lambda$

$10-30°$ during one rotation. Values of H_{t} and H_{r} were derived with the use of
expressions (4) and (5) for different symmetric longitudes. The insignificant
variations of H_{t} and H_{r} depending on the longitudes used indicate that we ha-
ve been justified in using equation (1).

3. RESULTS OF ANALYSIS OF SYNOPTIC MAPS OF THE TOROIDAL AND RADIAL
COMPONENTS OF THE LARGE-SCALE MAGNETIC FIELD

From the entire observational data set published in Solar Geophysical Da-
ta, we have chosen the series of magnetograms that involved the least number
of gaps in observations. The magnetograms thus selected cover the period from
February 1979 through October 1980. corresponding to the maximum and the be-
ginning of descent of the solar activity curve for cycle 21 as well as to the
time interval during which the polar magnetic field reverses its sign.

Figure 4 shows a series of daily magnetograms taken during the period in-
dicated above. Typical features of the evolution in the large-scale structure
of the magnetic field are evident. Early in the cycle, the structure was a ra-
ther simple one, with the magnetic field being negative in the northern hemi-
sphere and positive in the southern hemisphere. During the period under inves-
tigation the field structure has a very complicated character; sector structu-
re is well defined. Unipolar regions form sectors which extend throughout both
hemispheres. An opposite-polarity magnetic field is seen to gradually emerge
at the poles, as well as the confident reversal of the polar field by the be-
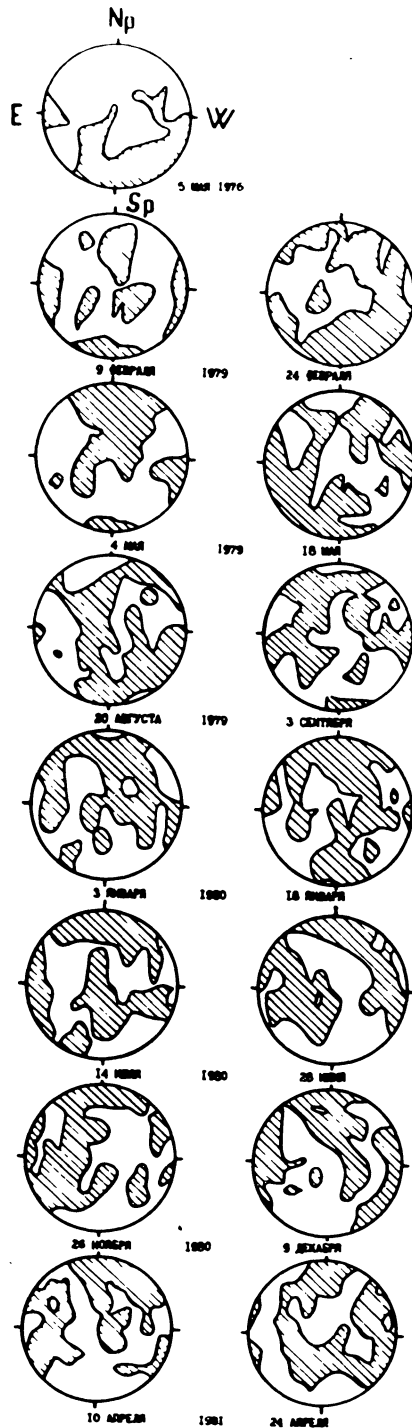ginning of 1980.

485

Fig. 4: The series of magnetograms characterizing the general evolution of the large-scale magnetic field from May 1976 through April 1981. The first magnetogram is taken from Duvall et al's (1979) paper and the

486

Fig. 4: remaining are from Solar Geophysical Data. Shaded areas correspond to
        the positive longitudinal field (antisunward direction of the field
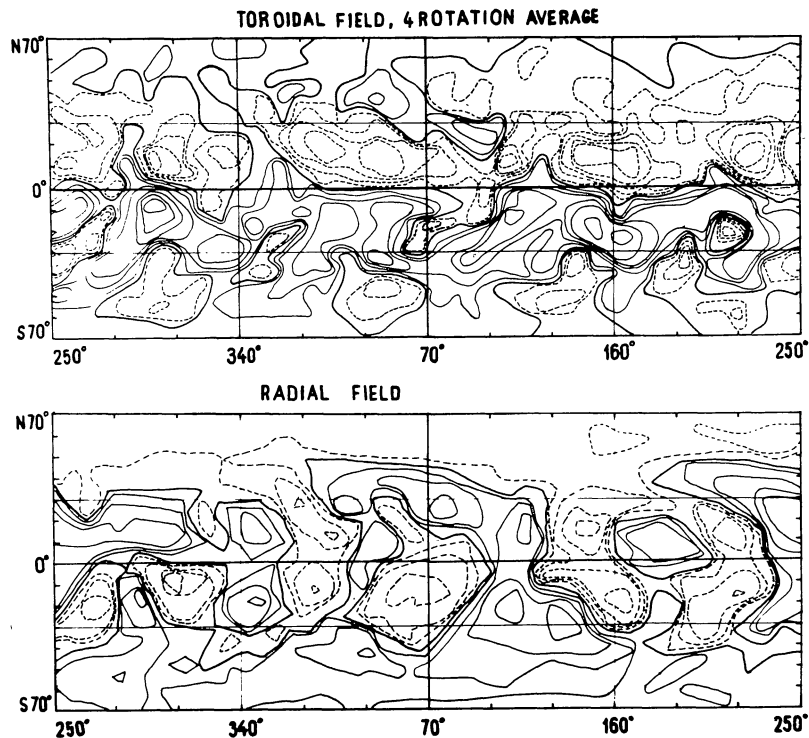   lines).

TOROIDAL FIELD, 4 ROTATION AVERAGE

RADIAL FIELD

Fig. 5: Synoptic maps of the toroidal and radial magnetic field. The isolines
        for the toroidal field correspond to 0, $\pm$ 25, $\pm$50, $\pm$100, $\pm$200, $\pm$400,
        and to $\pm$600 μT. The zeroth level is shown by a solid line. Dotted li-
        nes correspond to the direction of the toroidal field rfrom west to
        east and solid lines correspond to that from east to west. The isoli-
        nes for the radial field correspond to 0, $\pm$100, $\pm$200, $\pm$500, $\pm$1000,
        and to $\pm$2000 μT. The first solid line correspond to the zero line.
        Dotted lines correspond to the antisunward-directed field (-) and so-
        lid lines correspond to the sunward-directed field (+).
        This map has been obtained by averaging four seccessive synoptic maps
        for the period from 17 June to 7 September 1980.

    Figure 5 shows the structure of the mean toroidal and poloidal components
of the magnetic field. The synoptic map was obtained through averaging over
for solar rotations (17 June - 1 October 1980).
    The toroidal magnetic field covers the entire surface of the Sun. The
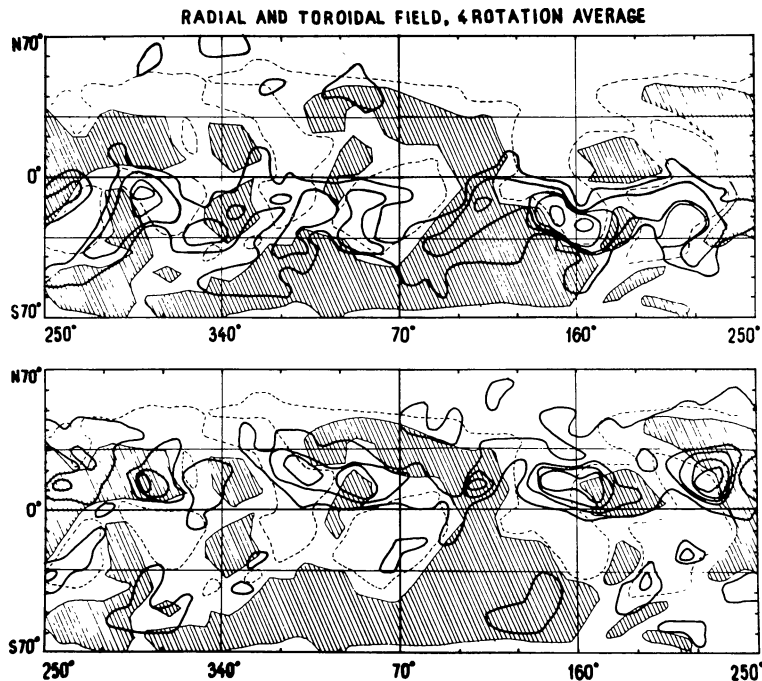preferential directions of the toroidal field in the S- and N-hemispheres are

487

RADIAL AND TOROIDAL FIELD, 4 ROTATION AVERAGE

Fig. 6: Synoptic maps of the toroidal and radial field, depicted in Fig. 5,
are superimposed. The E-W directed (upper map) and W-E directed (lo-
wer map) toroidal fields are marked separately. The isoline levels
for the toroidal field (solid heavy line) correspond to ±20, ±100,
±200, ±400, and to ±600 μ T. Shaded areas represent the radial
field with the lower level of +100 μ T. The dotted line correspon-
ds to the -100 μ T level.

opposite with respect to each other. The direction (from W to E in the N-hemi-
sphere and from E to W in the S-hemisphere) corresponds to subphotospheric
flux tubes which give rise to active regions of cycle 21. This result agrees
with the finding of Duvall et al. (1979) for the cycle onset.

   The distribution of toroidal field strength is non-uniform in longitude
and latitude. Figure 6 compares the synoptic maps of the toroidal and radial
magnetic fields. Hills of the toroidal field do not coincide with those of the
radial field and they show a tendency to displace into the region of the ra-
rial field zero line. This tendency is more clearly seen in maps for indivi-
dual rotations. We should like to emphasize the fact that the toroidal field
exists not only on Hall boundaries of polarity inversion of the large-scale
radial field but also on anti-Hall boundaries. As for Hall boundaries, it
might be expected that this is due to emergeing magnetic flux tubes. In order
to identify the magnetic field structure on anti-Hall boundaries let us look
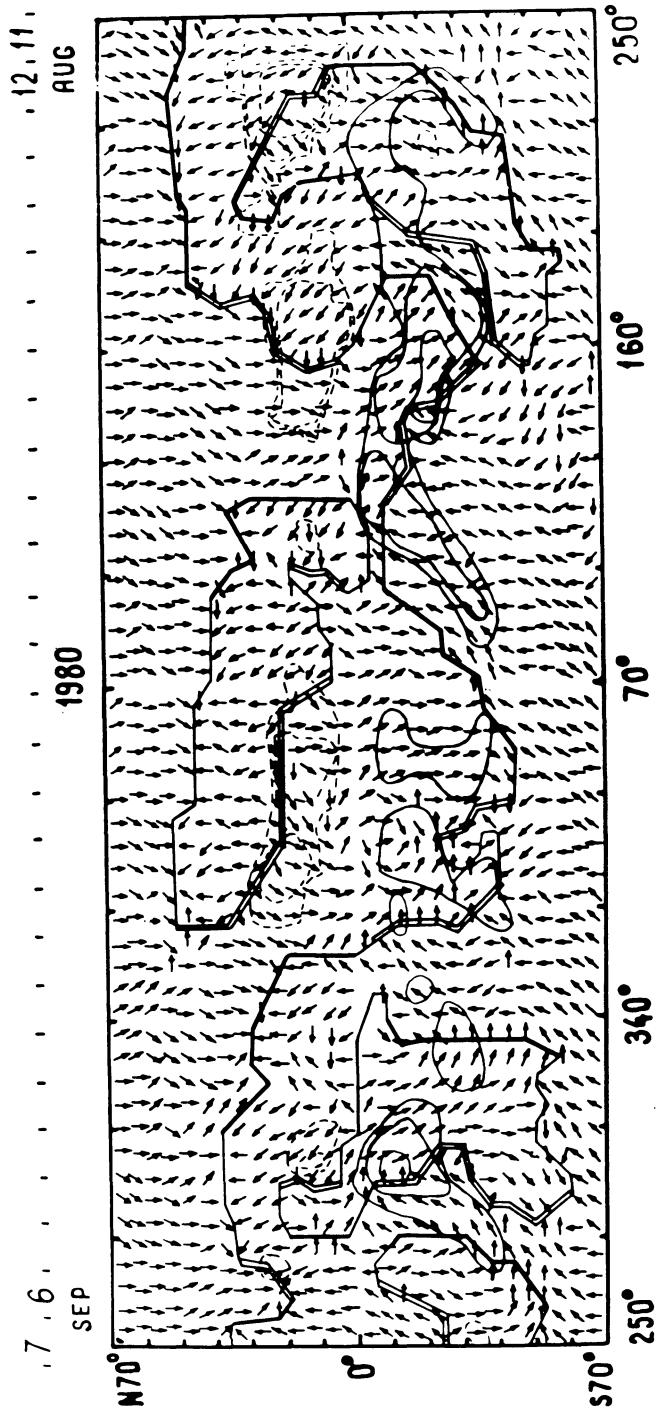at Figure 7 in which the arrows indicate the slope of the field vector with

488

Fig. 7: The synoptic map of the magnetic field full vector slope with respect to the radial direction (angle ∠ in Fig. 1) and the zero line of the radial field for one rotation from 10 August - 7 September 1980. The up- downward pointing arrow (↑↓) corresponds to ∠ = 0, i.e. there exists a purely radial field directed from the Sun or to the Sun. The different inclinations of the arrows correspond to the values of angle ∠ rounded-off to the nearest selected levels: 0°, 30°, 45°, 60°, and 90°. The solid line corresponds to the anti-Hall boundary and the double solid line corresponds to the Hall boundary.

489

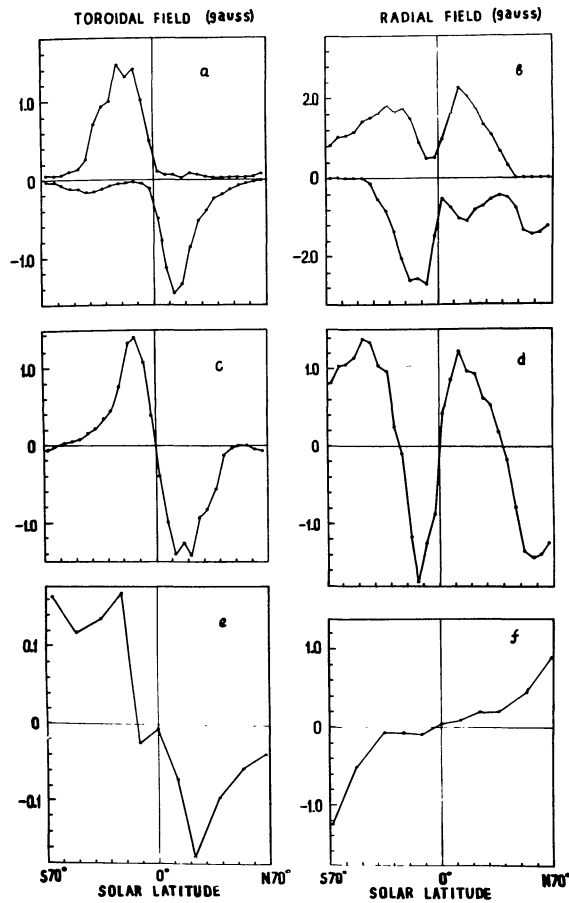TOROIDAL FIELD (gauss)   RADIAL FIELD (gauss)

Fig. 8: The latitude distribution of the toroidal and radial fields based on
synoptic maps presented in Fig. 5. Figures a and b present the toro-
idal and radial fields separately for each sign as a function of la-
titude. Figures c and d present the mean toroidal and radial fields
as functions of latitude. The curves in Figures c and d may be ob-
tained by adding together the curves in Figures a and b. Figures e
and f are taken from a paper by Duvall et al. (1979) and show the
latitude distribution of the mean toroidal and radial fields avera-
ged over the period May 1976 - June 1977.

respect to the solar radius as well as the field direction.

Hall boundaries of the large-scale magnetic field polarity inversion are
marked by a double line and anti-Hall boundaries are shown by a signale line.
The field vector directions clearly reveal on the Hall boundaries an arch-like
structure of field whereas on the anti-Hall boundaries an "anti-arch" structu-
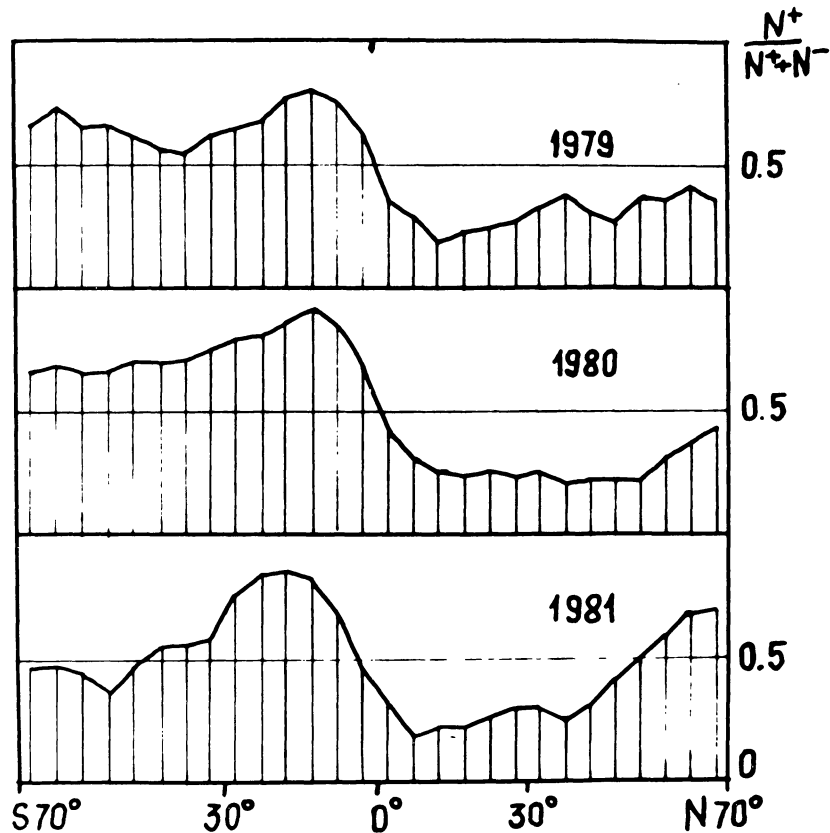re of field is observed. The magnetic field there looks like an inverted arch

490

$$\frac{N^+}{N^+ + N^-}$$

Fig. 9: The heliographic distribution of the sigh of the toroidal mean mag-
netic field for several solar rotations for three periods whose mid-
dles coincide with May 1979, June 1980 and May 1981. N^+ is the num-
ber of elements of a size of 5 x 5' degrees for the selected latitu-
de with the (+) sign of the toroidal field. N^- is the number of ele-
ments with the (-) sign.

which is open high in the atmosphere and is closed in photospheric and subpho-
tospheric layers.

The latitude distribution of the toroidal field (Figure 8) shows maxima
in both hemispheres at latitudes ± 15-$20°$. The mean field strength in the regi-
on of the maxima is 1 to 1.5 Gs. At the beginning of the cycle the mean field
strength there was 0.1 Gs. Earlier in the cycle, toroidal field maxima were
located at latitudes 30-40° in the N-hemisphere and within 30-70° in the S-he-
misphere (Duvall et al., 1979).

It is interesting to note a peculiar feature on the synoptic maps of the
toroidal field (Figure 5). At latitudes over 40° in both hemispheres there
appears a region of a weak toroidal field (of 0.05 to 0.1 Gs) with opposite
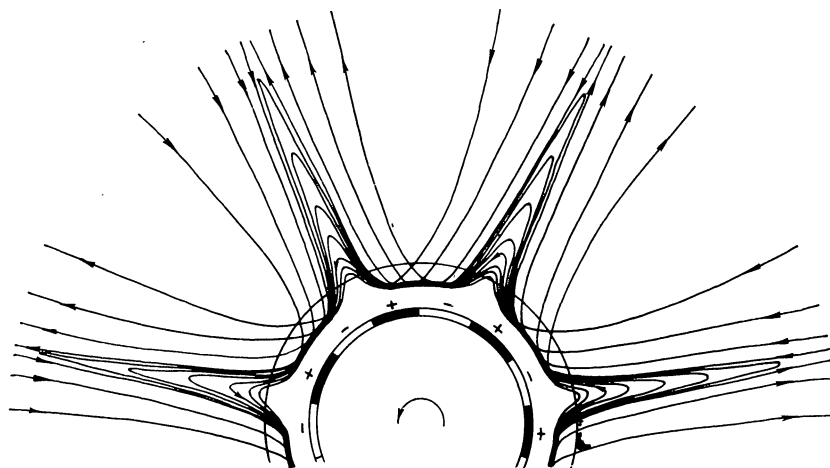
Fig. 10: A schematic representation of the structure of the large-scale magnetic field on the Sun. The transition from (-) to (+) is the Hall boundary and the transition from (+) to (-) is the anti-Hall boundary.

direction as compared with lower latitudes. The area of oppositely-directed toroidal field regions distinctly shows a tendency to increase at higher latitudes at the time the polar fields reverse. This tendency is well traceable in Figure 9 showing the plots of latitude distribution of sign of the mean toroidal magnetic field for three periods. The middles of these periods occur in May 1979, June 1980, and May 1981 (plots I, II and III, respectively). On the plots the Y-axis indicates values determined from

$$\frac{N^+}{N^+ + N^-}$$

where N^+ and N^- is the number of 5 x 5 degree elements of the surface respectively with positive and negative direction of the toroidal magnetic field. Therefore, shaded and non-shaded portions of the figure represent the areas occupied by opposite magnetic fields. From these plots it is quite evident that not only do the unipolar fluxes predominate in the S- and N-hemispheres but so do the areas occupied by unipolar fields.

The mean radial field strength at latitudes $0 \pm 30°$ varies from 1 to 2.5 Gs and the field direction coincides with the leading polarity over the cycle while at latitudes over $30°$ it coincides with the trailing polarity in their respective hemispheres.

The results we have obtained by analyzing the structure of the large-scale toroidal magnetic field of the Sun led us to an idea of the general structure of large-scale fields which may be visualized such as shown in Figure 10.

492

The observed toroidal field in the photosphere is associated with the global subphotospheric toroidal magnetic field of the Sun which is postulated in the Babcock-Leighton model (Babcock, 1961; Leighton, 1964). Emerging magnetic fluxes are observable as the toroidal component of field in the region of Hall boundaries of radial field polarity inversion.

The toroidal field in the region of anti-Hall boundaries reflects subphotospheric toroidal magnetic flux tubes which connect the leading to succeeding portions of neighbouring bipolar magnetic regions (BMO). Since the succeeding BMO regions are observed to be moving poleward and the leading BMO portions equatorward, this causes the subphotospheric toroidal fluxes to turn around and to produce a new poloidal field of opposite sign. The weak (about 0.1 Gs) toroidal field of opposite sign that was detected at high latitudes, is, possibly, associated with the fact that the newly formed poloidal field produces, as a result of differential rotation, a new toroidal field of the next 22nd activity cycle.

REFERENCES

Babcock, H.W.: 1961, Astrophys. J., 133, 572.
Duvall, T.L., Scherrerm P.H., Svalgaard, L., Wilcox, J.H.: 1979, Solar Phys., 61, 233.
Howard, R.: 1974, Solar Phys., 39, 275.
Leighton, R.B.: 1964, Astrophys. J., 140, 1547.
Svalgaard, L., Duvall, T.L., Scherrer, P.: 1978, Solar Phys., 58, 225.